SEMARAK ILMU PUBLISHING

Journal of Advanced Research in Numerical Heat Transfer

Journal homepage:
https://semarakilmu.com.my/journals/index.php/arnht/index
ISSN: 2735-0142

Analysis of the Effect of Tortuosity Porous Heatsink on Force Convection Heat Transfer

Imam Akbar[1], Dewi Rawani[1], Heriyanto Rusmaryadi[1], Martin Luther King[1], Pramadhony[1], Zulkarnain Fatoni[1] Ahmad Malik Abdul Aziz[2], Akbar Teguh Prakoso[3], Hasan Basri[3], Agung Mataram[3,*]

[1] Department of Mechanical Engineering, Faculty of Engineering, Tridinanti University, Palembang 30129, South Sumatra, Indonesia
[2] Department of Architecture, Faculty of Engineering, Tridinanti University, Palembang 30129, South Sumatra, Indonesia
[3] Department of Mechanical Engineering, Faculty of Engineering, Universitas Sriwijaya, Indralaya 30662, South Sumatra, Indonesia

ARTICLE INFO

Article history:
Received 8 October 2023
Received in revised form 10 November 2023
Accepted 9 December 2023
Available online 31 January 2024

Keywords:
Heatsink; tortuosity; force convection; computational fluid dynamics

ABSTRACT

The improvement of performance in modern electronic devices has driven rapid advancements in the field of thermal management. Excessive heating of electronic components can lead to damage and decreased device performance. This research aimed to analyze the effect of tortuosity porous heatsink on force convection heat transfer. Computational fluid dynamics methodology was used to model airflow and the distribution of temperature, velocity, convective heat transfer coefficient, and turbulence kinetic energy (TKE) in heatsinks with varying tortuosity levels. Results show that tortuosity has a positive linear correlation with heatsink surface area and pressure drop. However, it has a negative linear correlation with surface heat transfer coefficient (SHTC). When the tortuosity increases, the surface area increases from 9298.48 mm^2 to 12711.93 mm^2, and the pressure drop increases from 19.587 Pa to 24.296 Pa. By contrast, the surface heat transfer coefficient decreased significantly from 41.1214 $W\ m^{-2}\ K^{-1}$ to 30.8454 $W\ m^{-2}\ K^{-1}$. This study also shows that heatsinks with low tortuosity have a more uniform distribution of temperature, velocity, and TKE, resulting in higher cooling efficiency. Thus, we conclude that tortuosity is an important factor in heatsink design and optimization, and a suitable level of tortuosity should be achieved.

1. Introduction

The improvement of performance in modern electronic devices has driven rapid advancements in the field of thermal management. Excessive heating of electronic components can lead to damage and decreased device performance [1]. One common approach to address this heating issue is by utilizing heatsinks [2]. Heatsinks are vital components in cooling system designs aimed at dissipating the heat generated by electronic components, maintaining device temperatures, and enhancing performance [3].

* *Corresponding author.*
E-mail address: amataram@unsri.ac.id (Agung Mataram)

https://doi.org/10.37934/arnht.16.1.5769

In prior research, traditional manufacturing methods have been used to produce relatively simple heatsink shapes such as plate-fin [4], cylindrical fin [5,6], or pin-fin heatsinks [7]. However, with the development of additive manufacturing (AM) technology, researchers and designers now have access to more flexible production methods capable of creating more intricate structures [8], This opens up opportunities for increased surface area, reduced heatsink size and weight, as well as integration of heatsinks into more compact product designs and the creation of more efficient heat channels.

In heatsink design, geometric structure plays a crucial role in determining heat transfer efficiency [9]. Over the past decades, intensive research has been conducted to explore innovative and efficient heatsink structures. One type of structure that has garnered researchers' interest is the triply periodic minimal surface (TPMS) structure [10,11]. These structures offer unique geometric complexities and varying curvatures, and research results indicate that the TPMS heatsink object orientation, pin fins, and aluminum metal foam greatly affect the thermal performance of the heat sink. Therefore, TPMS heat sinks have better thermal performance than pin fin heat sinks by 35%–50% and aluminum metal foam heat sinks by 16%–44%. We argue that any change in the orientation of the heatsink tortuosity value can be different, thereby affecting the performance of the heatsink. Previous studies revealed that tortuosity, the ratio of the actual flow path length to the unobstructed flow path length, plays an important role in porous media for fluid flow. We also found that greater tortuosity tends to increase surface area [12,13]. Thus, we hypothesize that a higher tortuosity value results in a greater available heatsink surface area to transfer heat to the surrounding medium. However, increased tortuosity can also lead to higher hydraulic resistance, thereby reducing airflow through the heatsink and lowering the convective heat transfer coefficient.

In this context, this research aims to conduct a comprehensive numerical analysis of the influence of tortuosity in gyroid, diamond, split P, and Fin structures on heat transfer using forced convection heatsinks. Computational fluid dynamics (CFD) methodology is used to model airflow around the heatsinks and analyze temperature distribution, airflow velocity, and convective heat transfer coefficients with varying tortuosity in four heatsink structures. This research holds significant objectives. First, an in-depth numerical analysis provides a deeper understanding of the effect of tortuosity on heat transfer using forced convection heatsinks with gyroid, diamond, and split P structures. These results offer valuable insights for cooling system designers and engineers in developing more efficient heatsinks with optimal capabilities to effectively transfer heat from electronic components to the environment. Second, this research enables the identification of the most optimal heatsink structure to address electronic component overheating issues, thereby enhancing the overall electronic device performance.

With a better understanding of factors influencing tortuosity and heat transfer in heatsinks, this research contributes significantly to the development of more efficient cooling technologies for electronic applications. given the objectives, namely numerical analysis of the effect of tortuosity of heatsink fins, gyroids, diamonds, and splitP on force convection heat transfer. The results can serve as a basis for designing a relatively optimal heatsink with appropriate tortuosity to reduce excessive heating of electronic components. As a result, this research expected to positively affect the advancement of sophisticated and reliable electronic technology.

2. Methodology

2.1 Hetsink Design

In this research, the development of heatsink design was carried out using generative modeling techniques involving algorithms to produce complex geometric structures through the nTopology

software version 3.43.31. The schematic of the heatsink design for gyroid, diamond, and splitP structures is shown in Figure 1. The first stage involves creating models of pillars, plates, and boxes. The second stage involves applying the rectangular volume lattice feature to the box, where diamond and gyroid unit cells are selected. In the third stage, the "remap cylinder field" feature is applied to alter the position of each point in a plane based on cylinder surfaces. In addition, this remap feature assists the researchers in controlling the thickness of unit cells in various parts of the structure when their performance is unsatisfactory during the simulation process. Moreover, this thickness can be controlled to determine the level of structural porosity. The final stage involves applying the Boolean union feature to the plate and pillar with a blending radius of 0.5 mm.

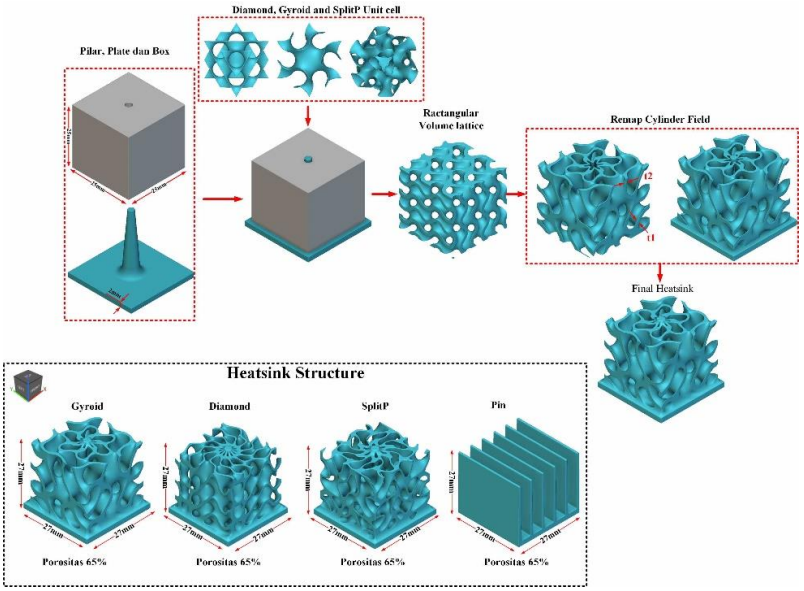

Fig. 1. Schematics diagrams heatsink design

Based on the heatsink design in Figure 1, the thickness values used in the proposed design to achieve uniform porosity, which is 65%, throughout the heatsink design are shown in Table 1.

Table 1
Dimensional parameters of the heatsink design

Heatsink structure	Thickness [mm]		Total volume (mm^3)	Heatsink volume (mm^3)	Porosity (%)
	t1	t2			
Gyroid	1	0.5	20384	6940.9	65.9
Diamond	0.9	0.3	20384	6980.3	65.8
SplitP	0.9	0.3	20384	6951.7	65.9
Fin	1.09	0.9	20384	6955.9	65.9

2.2 Tortuosity and Pore Size Measurement

In this research, to measure diffusion tortuosity and pore size in the CAD heatsink model, the design was exported to stereolithography (STL) format and imported into the slicing software (ChiTuBox, CBD-Tech) with a layer thickness of 0.05 mm, resulting in 426 slices with a resolution of 524 pixels. Furthermore, the heatsink pore size was measured using the bone J plugin from Fiji (Image J, NIH), through the following steps: (i) Brightness adjustment, (ii) Application of a threshold, and (iii) Removal of noise using the "remove outlier" function. Subsequently, the processed images were

exported in TIFF format and re-imported into the MATLAB software (MathWorks Inc.) using the Taufactor plugin. This method uses the finite difference method (FDM), where image voxels are used as a mesh for discretization in the simulation [14,15]. For accurate calculations, appropriate voxel sizes were input to ensure that the length, width, and height matched the actual dimensions. Based on the results of tortuosity and pore size measurements, the characteristic design of the heatsink is presented in Figure 2 and Table 2.

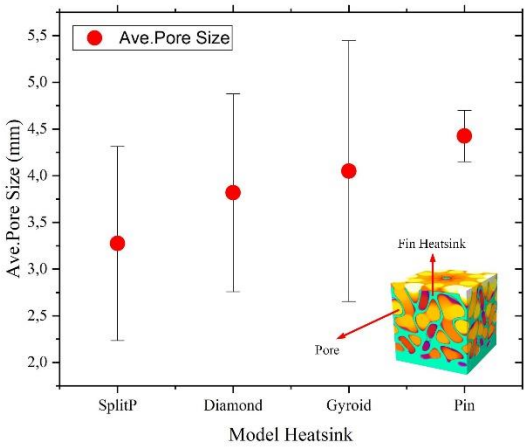

Fig. 2. Pore size heatsink structure

Table 2
Characteristics heatsink design

Heatsink structure	Surface area (mm^2)	Tortuosity
Gyroid	9871.02	1.74
Diamond	11929.04	1.78
SplitP	12711.93	2.46
Fin	9298.48	1

2.3 Computational Fluid Dynamics (CFD) Boundary Condition

In this research, CFD is used through the ANSYS software with a pressure-based solver and turbulence flow model to simulate heat transfer in a heatsink. The heatsink is made of aluminum [16], whereas the fluid used is air with an incompressible ideal gas model, possessing specific properties outlined in Table 3. The boundary conditions applied in this simulation encompass an incoming air flow of 0.00218 kg/s, with the outlet set at zero pressure. Furthermore, the wall sides are considered adiabatic no-slip boundaries with an ambient temperature of 300 K. For the heatsink base, we applied a heat flux with a value of 18750 W/cm^2 [17]. Information regarding all boundary conditions are presented in Figure 3A. Moreover, the polyhedral mesh is used to generate mesh for solid and fluid regions, as shown in Figure 3B. A conformal mesh should be mapped at the fluid/solid interface to ensure a conjugate heat transfer mechanism. The mesh is aggregated toward the denser zone using a prism layer mesh. Fine prism layers capture boundary layer phenomena for turbulence models that support sublayer thicknesses near the interface boundary.

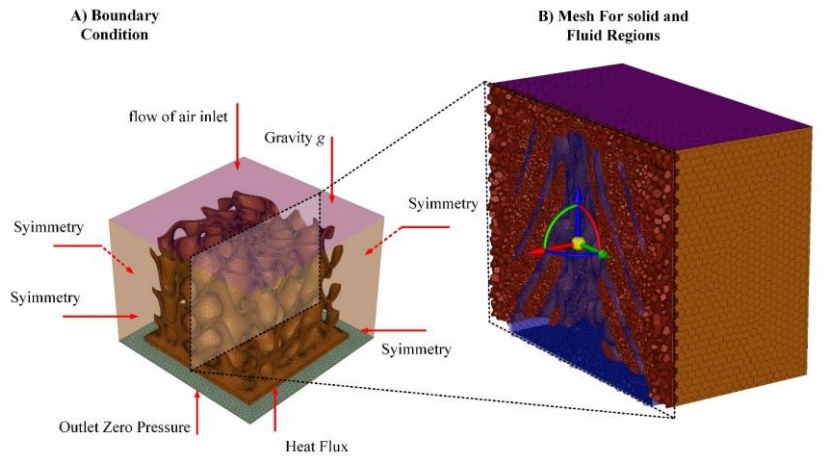

Fig. 3. A) Simulation boundary condition and B) mesh

Table 3
Air and aluminum properties

Heatsink structure	Density (kg/m3)		Cpecific heat (J/kg K)		Thermal conductivity (W/m K)		Air viscocity (kg/m s)
	Aluminum	Air	Aluminum	Air	Aluminum	Air	
Gyroid	2719	1.225	871	1006.43	202.4	0.0242	1.79E-05
Diamond	2719	1.225	871	1006.43	202.4	0.0242	1.79E-05
split	2719	1.225	871	1006.43	202.4	0.0242	1.79E-05
Fin	2719	1.225	871	1006.43	202.4	0.0242	1.79E-05

2.4 Governing Equations

The modes used in this research include heat conduction from the heat source to the heatsink fins and heat convection from the heatsink fins to the fluid. The equations governing these physical phenomena are the Naiver–Stokes momentum equation and the energy equation [18].

2.4.1 Equation of continuity

The equation of continuity can be written as follows [19]:

$$\frac{\partial u}{\partial x}+\frac{\partial v}{\partial y}+\frac{\partial w}{\partial z}=0 \tag{1}$$

2.4.2 Momentum equation

The momentum equations in the *x*, *y*, and *z* directions can be written as follows [16]:

$$u\frac{\partial u}{\partial x}+v\frac{\partial u}{\partial y}+w\frac{\partial u}{\partial z}=-\frac{1}{\rho}\frac{\partial p}{\partial x}+\nu\left[\frac{\partial^2 u}{\partial x^2}+\frac{\partial^2 u}{\partial y^2}+\frac{\partial^2 u}{\partial z^2}\right] \tag{2}$$

$$u\frac{\partial u}{\partial x}+v\frac{\partial u}{\partial y}+w\frac{\partial u}{\partial z}=-\frac{1}{\rho}\frac{\partial p}{\partial y}+\nu\left[\frac{\partial^2 v}{\partial x^2}+\frac{\partial^2 v}{\partial y^2}+\frac{\partial^2 v}{\partial z^2}\right] \tag{3}$$

$$u\frac{\partial u}{\partial x}+v\frac{\partial u}{\partial y}+w\frac{\partial u}{\partial z}=-\frac{1}{\rho}\frac{\partial p}{\partial z}+\nu\left[\frac{\partial^2 w}{\partial x^2}+\frac{\partial^2 w}{\partial y^2}+\frac{\partial^2 w}{\partial z^2}\right]-g_z \tag{4}$$

where ρ is the fluid density, p is the pressure within the fluid, v is the kinematic viscosity, g is the gravitational acceleration and (u, v and w) represent the velocity vector components in the x, y, and z directions.

2.4.3 Energy equation

The energy equation for the fluid can be written as follows [19]:

$$\rho c_p \, u\frac{\partial T}{\partial x} + \rho v\frac{\partial T}{\partial y} + \rho w\frac{\partial T}{\partial z} = \frac{\partial p}{\partial y} + \mu\left[\frac{\partial^2 T}{\partial x^2} + \frac{\partial^2 T}{\partial y^2} + \frac{\partial^2 T}{\partial z^2}\right] \quad (5)$$

2.4.4 Surface heat transfer coefficient

The surface heat transfer coefficient, can be calculated as follows [20]:

$$q_w^{"} = -k\frac{dt}{dy} \quad (6)$$

$$Q = q_w^{"}A \quad (7)$$

$$Q = hA(T_w - T_\infty) \quad (8)$$

$$h = \frac{Q}{A(T_w - T_\infty)} \quad (9)$$

where *K* is the thermal conductivity, $q_w^{"}$ is the heat flux received by the wall, *Q* is the total heat received by the wall, *h* is the convective heat transfer coefficient between the wall and the surrounding fluid, *A* is the surface area, T_w is the wall temperature, and T_∞ is the fluid temperature surrounding the wall.

3. Results and Discussion

In this research, our main objective is to further investigate the impact of varying levels of tortuosity on the thermal performance of heatsinks with different structures, such as gyroid, diamond, splitP, and fin. The method used involves a series of FDM simulations to measure the tortuosity levels within each heatsink structure, along with CFD simulations to visualize the airflow through the heatsinks exposed to a constant heat flux. With this approach, we aim to acquire relevant data, especially surface heat transfer coefficient values.

Our research findings in Figure 4A, show that a linear correlation exists between the tortuosity level and the heatsink surface area with a coefficient of determination R^2= 0.63. This result indicates that changes in tortuosity have a consistent impact on the heatsink surface area. As the tortuosity level increases, the heatsink surface area also significantly increases, ranging from 9298.48 mm^2 to 12711.93 mm^2. This discovery aligns with prior research [12], which indicated the presence of a specific phase, where an increase in tortuosity correlates with an increase in heatsink surface area.

In general, tortuosity is a measure that describes how winding or meandering a surface is [21] a higher tortuosity indicates greater distance that air must travel along the heatsink surface. Numerous studies have examined the impact of surface area by extending the size of heatsink fins on heatsink thermal management, as proposed by Subramani *et al.,* [22] They stated that a larger surface area in

the same heatsink design case increases the heat transfer coefficient due to the increased contact between the fluid and the heatsink, leading to thermal diffusion and convection.

However, the interesting aspect in our research is the significant impact of tortuosity levels on pressure drop as depicted in Figure 4B. The results of linear regression analysis with a coefficient of determination R^2=0.75 indicate that a higher tortuosity level, results in greater increase in pressure drop. The range of pressure drop varies from 19.587 to 24.296 Pa. This phenomenon is causing by factors such as pore size [23] and tortuosity level itself. High tortuosity levels result in increased friction between the fluid and the heatsink surface, ultimately creating turbulent conditions in the fluid flow. Turbulence is a state in which fluid flow becomes irregular and moves randomly. This effect, in turn, can lead to energy loss in the fluid flow, contributing to the increase in pressure drop.

Understanding the impacts of factors, such as tortuosity and pressure drop, is crucial, considering the importance of heatsink thermal performance, especially in applications involving significant airflow. High pressure drop levels can lead to energy losses and generate noise in the airflow system. Therefore, optimization efforts are necessary in heatsink design and geometry to achieve high cooling efficiency while maintaining minimal pressure drop.

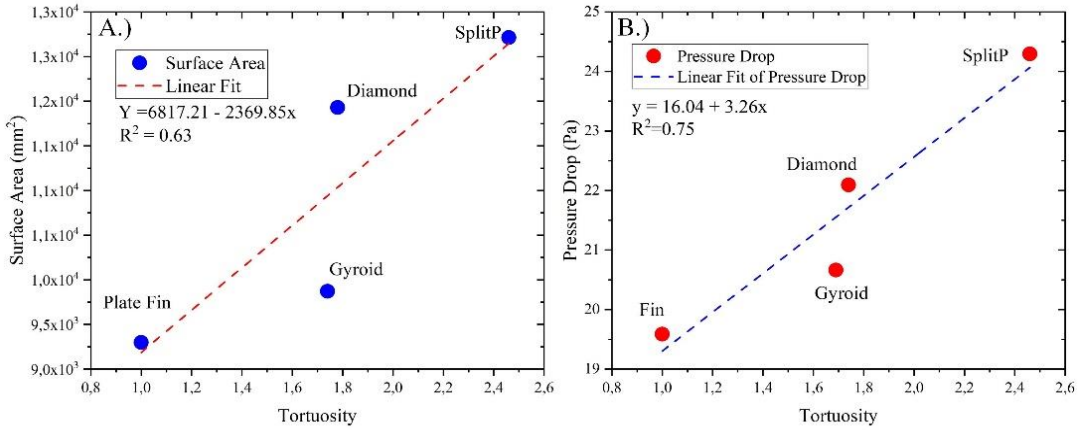

Fig. 4. Relationship between tortuosity with A) surface area and B) Pressure Drop heatsink

The results of this simulation are presented in Figure 5, illustrating the relationship between tortuosity and the surface heat transfer coefficient (SHTC) value on the heatsink. This relationship can be predicted with significant accuracy by using linear regression, as indicated by the coefficient of determination value R^2=0.88. This signifies that variations in the surface heat transfer coefficient due to changes in tortuosity. The analysis results, uncover that higher levels of tortuosity correspond to lower SHTC values. This outcome implies that as the tortuosity of the heatsink increases within the range of 1 to 2.46, the SHTC value significantly decreases from 41.1214 W m^{-2} K^{-1} to 30.8454 W m^{-2} K^{-1}. This change demonstrates a strong negative correlation between tortuosity level and heat transfer efficiency, measured through SHTC.

The decrease in SHTC on the heatsink with higher tortuosity levels can be explained by several factors. An increase in tortuosity leads to a smaller, more complex, and winding average airflow path or pore size, as observed in Figure 2. The main impact is the thickening of the boundary layer of air along the heatsink's surface. This thicker boundary layer hinders the heat transfer between the surface and the airflow due to frictional forces between the fluid and the heatsink, resulting in a reduced temperature gradient within the boundary layer. A low temperature gradient indicates a low heat transfer rate. Furthermore, the heat conduction within the boundary layer is much weaker than the direct heat convection [24]. This phenomenon is reinforced in this research, as presented in Figure 6, where the temperature difference on pin fin structures is significantly higher, pproximately

27.24 K, than the TPMS structures such as gyroids with a value of 25.38 K, diamonds with a value of 23.83 K, and splitP with a value of 22.76 K. In addition, increasing tortuosity also tends to enhance turbulence in the airflow. While turbulence can generally aid in mixing the boundary layer and improving heat transfer, at extreme levels, excessive turbulence can disrupt efficient laminar flow and overall reduce heat transfer.

In general, high tortuosity increases the surface heat transfer coefficient on the heatsink because the air flowing along the fins or pins of the heatsink experiences turbulence, enhancing mixing and convective heat transfer between the air and the heatsink surface [25]. This condition can improve heatsink cooling efficiency and reduce the temperature of electronic components. However, excessively high tortuosity can also decrease the surface heat transfer coefficient on the heatsink because air flowing along extremely convoluted fins or pins may experience increased pressure and viscosity, leading to decreased airspeed and Reynolds numbers [26]. This phenomenon can result in a transition from turbulent to laminar flow, reducing mixing and convective heat transfer between the air and the heatsink surface. Thus, heatsink cooling efficiency is decreased, and the temperature of electronic components is increased.

The findings of this study hold significant implications for efficient heatsink design. While higher levels of tortuosity is expected to enhance heat transfer due to the convoluted airflow, these findings indicate the opposite. Increasing tortuosity levels actually reduce heat transfer efficiency, which could detrimentally impact the overall system performance. Therefore, optimal heatsink design should consider a balance between surface complexity (tortuosity) and heat transfer capability (SHTC).

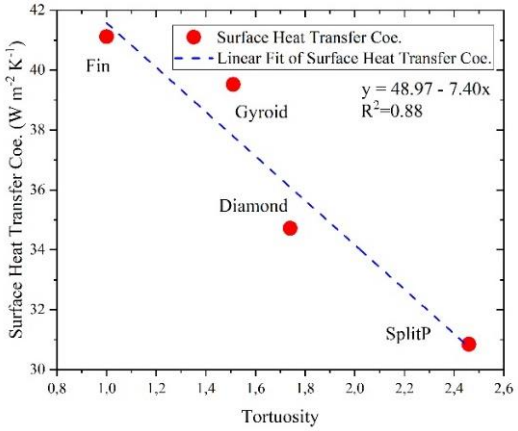

Fig. 5. Relationship between tortuosity and surface heat transfer coefficient heatsink

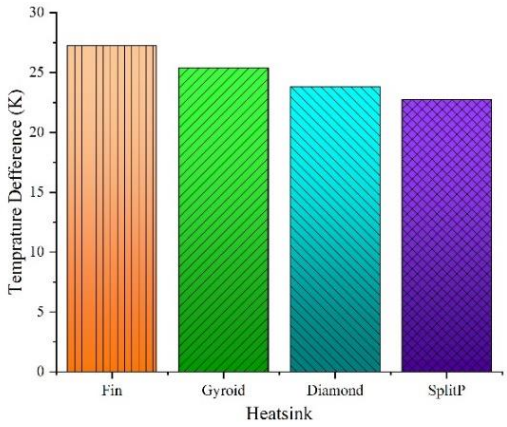

Fig. 6. Temperature difference heatsink structure

Figure 7 provides a visual representation of the temperature distribution on each heatsink structure. In the image, the blue color indicates the minimum temperature set at 55°C, and the red color indicates the maximum temperature at 61°C. These results, indicate that the fin and gyroid structures with higher red color intensity, exhibit higher temperatures in those areas. Conversely, areas with diamond and splitP structures tend to have higher blue color intensity, indicating lower temperatures. Even temperature distribution across the heatsink is a crucial factor in maintaining the performance of an electronic system or a device that requires cooling. This study suggests that the fin and gyroid structures exhibit more uniform temperature distributions than the diamond and splitP structures.

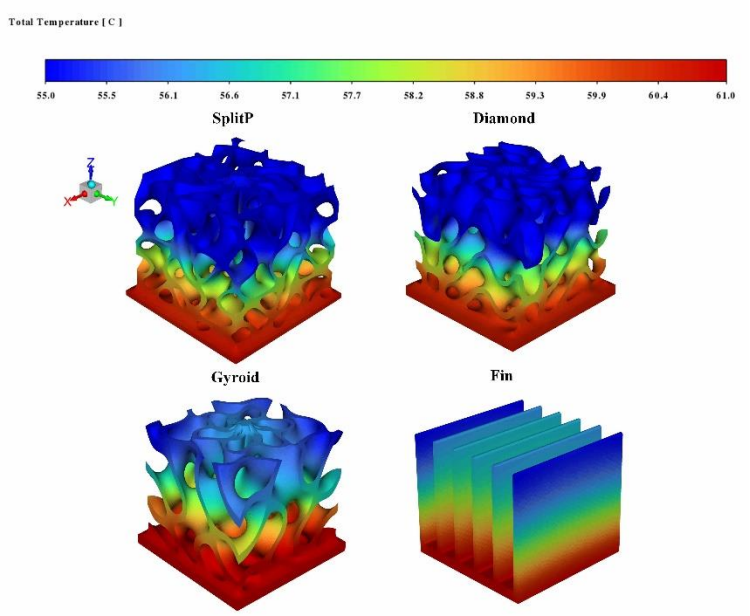

Fig. 7. Total temprature distribution on heatsink structure

In this research, numerical simulations are conducted to understand the behavior of airflow through heatsink structures with various levels of tortuosity. The simulation results provide insights into how airflow behaves through different types of heatsink structures, affecting heat transfer efficiency. In Figure 8, the distribution of airflow velocity is displayed using a color scale, where blue represents minimum velocity (0 m/s) and red represents maximum velocity (6 m/s). Through this analysis, we can identify the patterns of airflow formed within the heatsink structures with varying levels of tortuosity.

Heatsink structures with low tortuosity levels, such as fin and gyroid, exhibit more uniform velocity distributions. The airflow tends to flow more smoothly and with minimal disturbances. This even velocity distribution enables accumulated heat on the heatsink surface to be efficiently transferred to the surrounding air. This directly contributes to cooling efficiency. On the other hand, heatsink structures with high tortuosity levels, like diamond and splitP, display uneven velocity distributions. Within the heatsink pores, numerous significant changes in velocity and direction occur. The airflow becomes obstructed in certain areas while moving faster in others. As a result, regions with less effective airflow are formed, leading to excessive heating in certain heatsink areas due to inadequate air circulation.

Heatsink structures with even velocity distributions tend to be more efficient in cooling the heat surface. Heat transfer efficiency increases because the air in direct contact with the hot surface is replaced more rapidly by cooler air. Conversely, in structures with uneven velocity distributions, some parts of the heatsink might not receive sufficient airflow to maintain safe temperatures [27]. This condition can decrease cooling efficiency and potentially endanger components that require cooling.

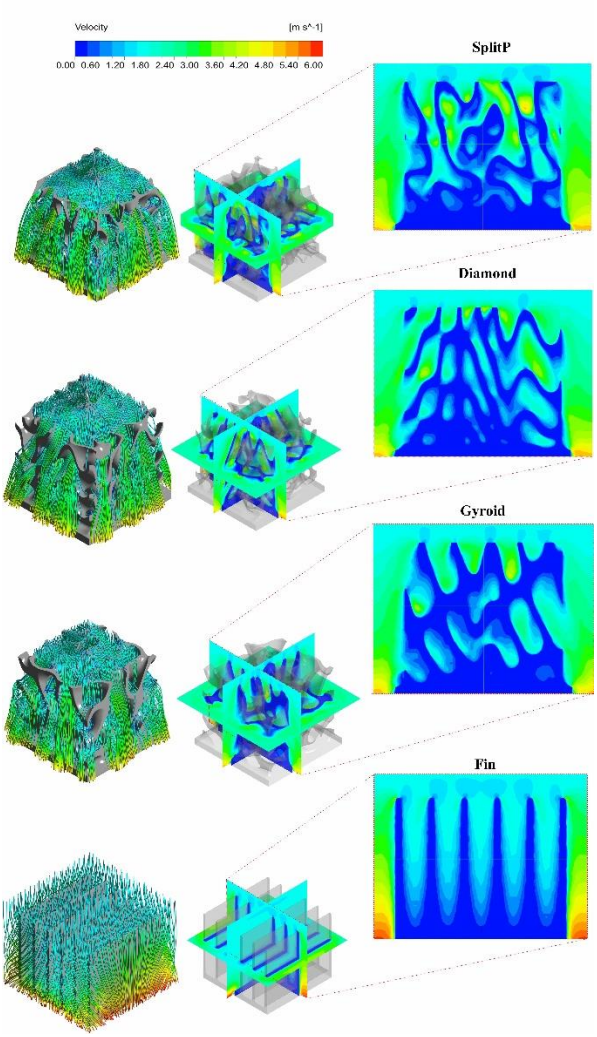

Fig. 8. Velocity distribution on heatsink

In the field of thermal and fluid engineering, turbulent flow analysis and the distribution of turbulence kinetic energy (TKE) play a crucial role in understanding and designing components, such as heatsinks [28]. Heatsinks are essential devices for heat management in various applications, including computer cooling, heating systems, and industrial machinery. The distribution of TKE around a heatsink provides profound insights into the characteristics of airflow and the cooling efficiency that can be achieved. TKE is a measure of kinetic energy associated with velocity variations within turbulent flow. In turbulent flow, air particles move randomly in various directions and speeds. TKE reflects these fluctuations in kinetic energy and is a significant indicator of turbulence intensity within the flow. TKE analysis allows us to understand the strength of air velocity changes in turbulent flow and how that energy is distributed in space.

Figure 9 illustrates the distribution of TKE around heatsinks with various geometries, including split P, diamond, gyroid, and fin structures. This TKE distribution shows how turbulent energy is dispersed around the heatsink in different shapes and surface areas. Upon observation, split P, diamond, and gyroid structures tend to have more TKE than the fin structure. This finding is evident from the darker colors on these structures in the visual representation. The primary reason behind this difference lies in the sudden shape changes within the split P, diamond, and gyroid structures. Abrupt changes in shape and surface can lead to significant variations in airflow direction and changes in air velocity around them, thereby creating zones of intensified turbulence and, consequently, generating more turbulent energy or TKE.

This finding holds significant implications for heatsink design. Heatsink structures with surface areas featuring abrupt shape changes, such as split P, diamond, and gyroid, tend to create greater resistance to airflow. In general, higher TKE value indicates higher turbulence intensity, indicating greater exchange of mass and energy between the fluid and the surface. This condition can increase the convective heat transfer coefficient and the rate of heat transfer from the heatsink to the air. However, the TKE value is also influenced by other factors, such as atmospheric stability, wind speed, and temperature gradient [29], [30]. However, at extreme levels, excessive turbulence can disrupt efficient laminar flow and reduce overall heat transfer.

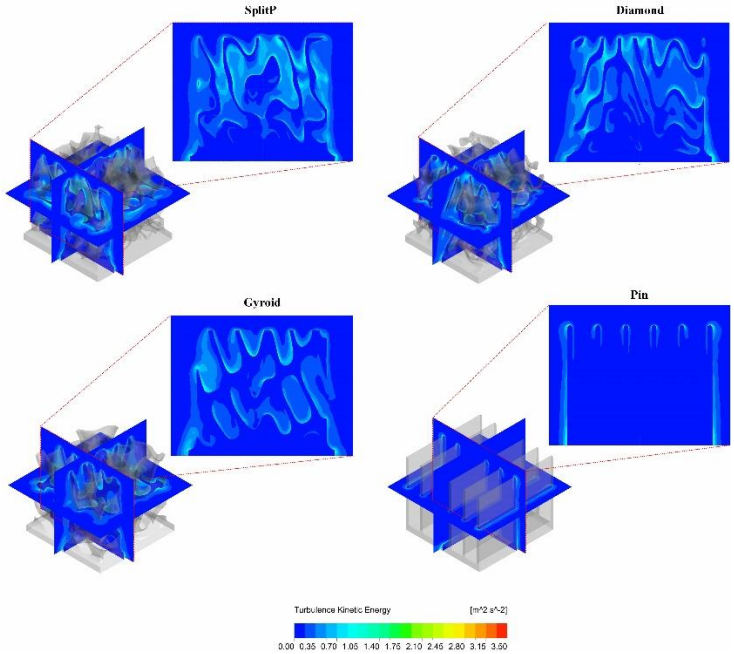

Fig. 9. Turbulence kinetic energi on heatsink

4. Conclusions

This paper presents a numerical analysis of the effect of tortuosity on heat transfer in heatsinks with different structures, such as gyroid, diamond, split P, and fin. CFD is used to simulate airflow and temperature distribution on the heatsink. The results show that tortuosity has a positive linear correlation with heatsink surface area and pressure drop, but it has a negative linear correlation with surface heat transfer coefficient (SHTC). When tortuosity increases, the surface area increases from 9298.48 mm^2 to 12711.93 mm^2, and the pressure drop increases from 19.587 Pa to 24.296 Pa. In contrast, the surface heat transfer coefficient decreased significantly from 41.1214 W m^{-2} K^{-1} to 30.8454 W m^{-2} K^{-1}. This study also shows that heatsinks with low tortuosity have a more uniform distribution of temperature, velocity, and TKE, resulting in higher cooling efficiency. Thus, we conclude that tortuosity is an important factor in heatsink design and optimization, and a suitable level of tortuosity should be considered to achieve efficient heat dissipation in electronic applications. This research contributes to the development of more advanced and reliable cooling technologies for electronic devices.

References

[1] Almubarak, Adel Ahmed. "The effects of heat on electronic components." *Int. J. Eng. Res. Appl* 7, no. 5 (2017): 52-57. https://doi.org/10.9790/9622-0705055257

[2] Hoque, Muhammad Jahidul, Alperen Günay, Andrew Stillwell, Yashraj Gurumukhi, Robert CN Pilawa-Podgurski, and Nenad Miljkovic. "Modular heat sinks for enhanced thermal management of electronics." *Journal of Electronic Packaging* 143, no. 2 (2021): 020903. https://doi.org/10.1115/1.4049294

[3] Zhou, Jinzhi, Xiaoling Cao, Nan Zhang, Yanping Yuan, Xudong Zhao, and David Hardy. "Micro-channel heat sink: a review." *Journal of Thermal Science* 29 (2020): 1431-1462. https://doi.org/10.1007/s11630-020-1334-y

[4] Sarap, Martin, Ants Kallaste, Payam Shams Ghahfarokhi, and Toomas Vaimann. "Analysis of Advanced Passive Heatsinks For Electrical Machines Enabled by Additive Manufacturing." In *2023 IEEE Workshop on Electrical Machines Design, Control and Diagnosis (WEMDCD)*, pp. 1-6. IEEE, 2023. https://doi.org/10.1109/WEMDCD55819.2023.10110940

[5] Özdilli, Özgür. "Design and thermal performance analysis of different type cylindrical heatsinks." *International Journal of Thermal Sciences* 170 (2021): 107181. https://doi.org/10.1016/j.ijthermalsci.2021.107181

[6] Kore, Sandeep S., Rupesh Yadav, Satish Chinchanikar, Pralhad Tipole, and Vishal Dhole. "Experimental investigations of conical perforations on the thermal performance of cylindrical pin fin heat sink." *International Journal of Ambient Energy* 43, no. 1 (2022): 3431-3442. https://doi.org/10.1080/01430750.2020.1834451

[7] Zapach, Trevor, Todd Newhouse, Jeff Taylor, and Peter Thomasing. "Experimental verification of a model for the optimization of pin fin heatsinks." In *ITHERM 2000. The Seventh Intersociety Conference on Thermal and Thermomechanical Phenomena in Electronic Systems (Cat. No. 00CH37069)*, vol. 1, pp. 63-69. IEEE, 2000.

[8] White, Andrew Scott, David Saltzman, and Stephen Lynch. "Performance analysis of heat sinks designed for additive manufacturing." In *International Electronic Packaging Technical Conference and Exhibition*, vol. 84041, p. V001T07A003. American Society of Mechanical Engineers, 2020. https://doi.org/10.1115/IPACK2020-2532

[9] Silva, Eva C., Álvaro M. Sampaio, and António J. Pontes. "Evaluation of active heat sinks design under forced convection—effect of geometric and boundary parameters." *Materials* 14, no. 8 (2021): 2041. https://doi.org/10.3390/ma14082041

[10] Baobaid, Nada, Mohamed I. Ali, Kamran A. Khan, and Rashid K. Abu Al-Rub. "Fluid flow and heat transfer of porous TPMS architected heat sinks in free convection environment." *Case Studies in Thermal Engineering* 33 (2022): 101944. https://doi.org/10.1016/j.csite.2022.101944

[11] Ali, Mohamed I. Hassan, Oraib Al-Ketan, Mohamad Khalil, Nada Baobaid, Kamran Khan, and Rashid K. Abu Al-Rub. "3D printed architected heat sinks cooling performance in free and forced convection environments." In *Heat Transfer Summer Conference*, vol. 83709, p. V001T09A012. American Society of Mechanical Engineers, 2020. https://doi.org/10.1115/HT2020-9067

[12] Prakoso, Akbar Teguh, Hasan Basri, Dendy Adanta, Irsyadi Yani, Muhammad Imam Ammarullah, Imam Akbar, Farah Amira Ghazali, Ardiyansyah Syahrom, and Tunku Kamarul. "The effect of tortuosity on permeability of porous scaffold." *Biomedicines* 11, no. 2 (2023): 427. ttps://doi.org/10.3390/biomedicines11020427

[13] Basri, Hasan, Akbar Teguh Prakoso, Zainal Abidin, Ardiansyah Syahrom, Imam Akbar, and Dendy Adanta. "The Effect of Tortuosity on Wall Shear Stress of Porous Scaffold." *CFD Letters* 15, no. 7 (2023): 61-73. https://doi.org/10.37934/cfdl.15.7.6173

[14] Cooper, Samuel J., Antonio Bertei, Paul R. Shearing, J. A. Kilner, and Nigel P. Brandon. "TauFactor: An open-source application for calculating tortuosity factors from tomographic data." *SoftwareX* 5 (2016): 203-210. https://doi.org/10.1016/j.softx.2016.09.002

[15] Fu, Jinlong, Hywel R. Thomas, and Chenfeng Li. "Tortuosity of porous media: Image analysis and physical simulation." *Earth-Science Reviews* 212 (2021): 103439. https://doi.org/10.1016/j.earscirev.2020.103439

[16] Kim, Dong-Kwon, Sung Jin Kim, and Jin-Kwon Bae. "Comparison of thermal performances of plate-fin and pin-fin heat sinks subject to an impinging flow." *International Journal of Heat and Mass Transfer* 52, no. 15-16 (2009): 3510-3517. https://doi.org/10.1016/j.ijheatmasstransfer.2009.02.041

[17] Freegah, Basim, Ammar A. Hussain, Abeer H. Falih, and Hossein Towsyfyan. "CFD analysis of heat transfer enhancement in plate-fin heat sinks with fillet profile: Investigation of new designs." *Thermal Science and Engineering Progress* 17 (2020): 100458. https://doi.org/10.1016/j.tsep.2019.100458

[18] Bataineh, Ahmad, Wafa Batayneh, Ahmad Al-Smadi, and Baian Bataineh. "Ladder Heat Sink Design Using Adaptive Neuro-Fuzzy Inference System (ANFIS)." *Financed by Scientific Research Support Fund* 13, no. 1 (2019): 27.

[19] Huang, Cheng-Hung, Jon-Jer Lu, and Herchang Ay. "A three-dimensional heat sink module design problem with experimental verification." *International Journal of Heat and Mass Transfer* 54, no. 7-8 (2011): 1482-1492. https://doi.org/10.1016/j.ijheatmasstransfer.2010.11.044

[20] Mohan, R., and P. Govindarajan. "Experimental and CFD analysis of heat sinks with base plate for CPU cooling." *Journal of mechanical science and technology* 25 (2011): 2003-2012. https://doi.org/10.1007/s12206-011-0531-8
[21] Rao, Dengyu, and Bing Bai. "Study of the factors influencing diffusive tortuosity based on pore-scale SPH simulation of granular soil." *Transport in Porous Media* 132 (2020): 333-353. https://doi.org/10.1007/s11242-020-01394-0
[22] Subramani, Shanmugan, and Mutharasu Devarajan. "Influence of extended surface area of heatsink on heat transfer: design and analysis." *Microelectronics International* (2023). https://doi.org/10.1108/MI-09-2022-0171
[23] Liu, Xiaobang, Yanxiang Li, Huawei Zhang, Yuan Liu, and Xiang Chen. "Effect of pore structure on heat transfer performance of lotus-type porous copper heat sink." *International Journal of Heat and Mass Transfer* 144 (2019): 118641. https://doi.org/10.1016/j.ijheatmasstransfer.2019.118641
[24] Grigull, Ulrich, and Heinrich Sandner. *Heat conduction*. Vol. 7. Berlin: Springer-Verlag, 1984. https://doi.org/10.1007/978-3-642-96816-7_2
[25] Ahn, J., Ephraim M. Sparrow, and John M. Gorman. "Turbulence intensity effects on heat transfer and fluid-flow for a circular cylinder in crossflow." *International Journal of Heat and Mass Transfer* 113 (2017): 613-621. https://doi.org/10.1016/j.ijheatmasstransfer.2017.05.131
[26] El-Okda, Yasser M., and Ghassan Nasif. "Conjugate Effect on the Heat Transfer Coefficient." *Journal of Advanced Research in Numerical Heat Transfer* 5, no. 1 (2021): 1-8.
[27] Saadoon, Zahraa H., Farooq H. Ali, Hameed K. Hamzah, Azher M. Abed, and M. Hatami. "Improving the performance of mini-channel heat sink by using wavy channel and different types of nanofluids." *Scientific Reports* 12, no. 1 (2022): 9402. https://doi.org/10.1038/s41598-022-13519-0
[28] Yeranee, Kirttayoth, and Yu Rao. "A review of recent investigations on flow and heat transfer enhancement in cooling channels embedded with triply periodic minimal surfaces (TPMS)." *Energies* 15, no. 23 (2022): 8994. https://doi.org/10.3390/en15238994
[29] Stull, Roland B. *An introduction to boundary layer meteorology*. Vol. 13. Springer Science & Business Media, 2012.
[30] Grošelj, Daniel, Christopher HK Chen, Alfred Mallet, Ravi Samtaney, Kai Schneider, and Frank Jenko. "Kinetic turbulence in astrophysical plasmas: waves and/or structures?." *Physical Review X* 9, no. 3 (2019): 031037. https://doi.org/10.1103/PhysRevX.9.031037